MLVis 2026: Machine Learning Methods in Visualisation for Big Data (2026)
D. Archambault, I. Nabney and J. Peltonen (Editors)

Integrating Gridded Glyph Maps and Self-Organizing Maps for Spatiotemporal Analysis

Julius Rauscher[1], Frederik L. Dennig[1], Udo Schlegel[2], Daniel A. Keim[1], and Tobias Schreck[3]

[1]University of Konstanz, Germany; [2]LMU & MCML Munich, Germany; [3]TU Graz, Austria

Abstract

Captured spatiotemporal data is increasing in size and complexity, requiring aggregation methods that preserve both spatial structure and temporal behavior. A central question is whether geographically proximate locations also exhibit similar temporal profiles, and where meaningful deviations from this expectation occur. We present a visual analytics approach that combines gridded glyph maps and self-organizing maps into a single superimposed representation, enabling interpolation between them. Our method supports a transition between spatially driven aggregation and similarity-driven grouping, enabling steering of the trade-off between spatial proximity and temporal similarity. To structure this analysis, we derive three task types from Tobler's First Law of Geography: confirming local similarity, detecting local deviation, and identifying remote similarity. We further complement the visual representation with measures of geographic nearness and temporal relatedness to filter cells and guide the interpolation process. A usage scenario using German COVID-19 incidence data illustrates the workflow in a real-world spatiotemporal analysis setting, revealing east-west regional differences and temporally similar urban dynamics across geographically distant locations.

CCS Concepts

• ***Human-centered computing*** → ***Visual analytics; Geographic visualization;***

1. Introduction

The growing size and resolution of spatiotemporal datasets require visual aggregation methods such as gridded glyphmaps [WHWC12] to support the analysis of how temporal behavior varies across space. A central principle for such analyses is articulated by Tobler's First Law of Geography: *"everything is related to everything else, but near things are more related than distant things"* [Tob70, p.236]. While this principle does not always hold, it provides a fundamental framework for analysis, where both the confirmation of this expectation and the identification of meaningful deviations from it are of interest. Andrienko et al. [AAB*10] introduce the complementary viewpoints of *space in time* and *time in space*. These perspectives are often conveyed through separate juxtaposed views [GCML06], which can introduce visual discontinuities between geographic and temporal structures. A superimposed visualization can alleviate this by coupling both perspectives in the same view. Gridded glyph maps provide such a superimposed visualization by aggregating data spatially and embedding temporal summaries directly in geographic space [CHM18, SRH23]. Their aggregation, however, is primarily driven by the spatial component.

A complementary perspective is provided by self-organizing maps (SOMs), which also aggregate data in a grid, but organize entities according to attribute similarity rather than geographic location [Koh82, GCS24]. SOM variants that incorporate geographic information have been studied [BLP05], but they do not provide an integrated visual representation that remains directly coupled to geographic space. We address this by combining SOM-based organization with a gridded glyph map in a single steerable superimposed visualization that enables continuous interpolation between spatially driven and attribute-similarity driven aggregation within a single visual interface. Our contributions are:

- An integrated **visual analytics approach** that combines geography-aware SOM organization with a gridded glyph map in a steerable superimposed view.
- A **measure-supported workflow** to investigate local agreement, local deviation, and remote similarity.
- A **usage scenario** on German COVID-19 incidence data illustrating the proposed workflow in practice.

2. Related Work

Gridded Glyphmaps – With IconMapper, Zhang and Pazner [ZP04] demonstrate how icons can serve as visualization primitives for a rasterized aggregation of multivariate spatial data. Wickham et al. [WHWC12] apply glyphmaps to spatiotemporal data using linear or circular linecharts, and further use line intensity or background coloring to encode the range. Other approaches further explore superimposed plots embedded in maps [GW15], value-scaled time-colored circles as aggregation glyphs [CHM18], and design alternatives for COVID-19 data [BDHL21]. Slingsby et al. [SRH23] use gridded glyphmaps to visualize inputs, outputs, and differences between spatial model runs. Laksono et al. [LSJ24] foster multicriteria decision analysis through an interface that allows the user to configure the grid layout and glyph design.

DOI: 10.2312/kjtgq,0.04/..3

While gridded glyphmaps provide a promising integrated solution for overview tasks of spatiotemporal data, they do not consider attribute similarity in their aggregation step and are all susceptible to the Modifiable Areal Unit Problem (MAUP) [Ope84], as the grid location is usually arbitrarily chosen.

Self Organizing Maps – Also known as Kohonen Maps [Koh82], SOMs are unsupervised machine learning methods for both clustering and dimensionality reduction that arrange similar data points in a cell grid. Many variations have been proposed to adapt the method to specific application scenarios [GCS24]. Bação et al. [BLP05] discuss SOM variants that account for spatial dependencies, either by adding spatial coordinates to the input vector, using hierarchical variants, or geographically limiting the search for the winning unit. Andrienko et al. [AAB*10] apply SOMs either to spatial situations or to temporal evolution profiles to facilitate orthogonal analytic perspectives that are embedded in a visual analytics framework. To investigate the influence of metadata properties such as location, Bernard et al. [BRS*12] propose a juxtaposed layout of a SOM grid and histograms. Hao et al. [HRJ*13] use SOMs to group statements from customer feedback into associations, and visualize these on a geographic map. Aside from geospatial applications, SOMs have been applied in object detection in videos [DYL*17], speech intonation research [SKB*18], or electron microscopy images [DPL*19].

Despite their visual similarities, SOMs have never been used in combination with geospatial gridded glyphmaps to the best of our knowledge. Instead, existing solutions often provide juxtaposed views rather than a single, integrated visual interface.

3. Integrating Gridded Glyph Maps and Self-Organizing Maps

As outlined in Sec. 2, gridded glyph maps and SOMs share intrinsic similarities, as both approaches perform an aggregation based on an underlying grid. While glyphmaps use the spatial information, SOMs typically leverage the attribute similarity. Both provide relevant viewpoints to investigate where and when Tobler's First Law of Geography applies [AAB*10], hence we propose an integrated visual analytics prototype that superimposes the spatial and temporal view and allows a fluid interpolation between the two variants. To structure the analysis process, we base our design decisions to support the investigation of the following scenarios based on Tobler's Law:

- **[T1] Confirm local agreement:** find geographically near locations with related temporal profiles.
- **[T2] Detect local deviation:** find geographically near locations with unrelated temporal profiles.
- **[T3] Detect remote similarity:** find geographically distant locations with related temporal profiles.

Nearness and Relatedness – To quantify Tobler's notion that nearby things tend to be related, we define two bounded cell-level measures. *Geographic nearness* captures whether the members of a cell also form a coherent local neighborhood in geographic space. *Temporal relatedness* captures whether the same members also form a coherent neighborhood in the feature space of temporal profiles. We formulate them as rank-based neighborhood measures, following prior work to characterize geographic neighborhood structures [GG06, RDS*25]. Let C be a cell with $n = |C|$ members, and let $\mathcal{N}^d(i)$ denote the n nearest neighbors of member $i \in C$ (including i itself) under Euclidean distance d; either d_{geo} over $(\text{lon}_i, \text{lat}_i)$ or d_{temp} over the temporal-profile vector p_i. We define

$$\kappa_d(C) = \frac{1}{n^2} \sum_{i \in C} |\mathcal{N}^d(i) \cap C|,$$

as the average fraction of each member's nearest neighbors that also belong to C. Sizing the neighborhood to n compares C against the most compact grouping of the same cardinality, so the score is directly interpretable without further normalization. Geographic nearness is $\kappa_{\text{geo}}(C)$ and temporal relatedness is $\kappa_{\text{temp}}(C)$. A value of 1 means C coincides exactly with the local neighborhood of each of its members, i.e., a perfectly compact group. Lower values indicate that members are intermingled with non-members, so C captures part of a broader area rather than an isolated cluster.

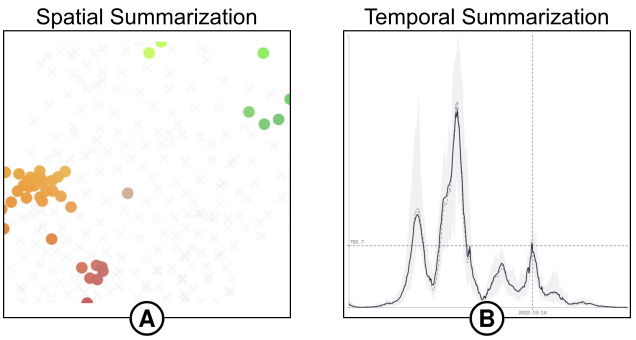

Figure 1: *(A) Showing the geographic arrangement of cell members within their bounding box; color encodes geographic position and gray points provide context from non-members. (B) Showing BMU (—), median (···), and interquartile range to summarize representative temporal behavior that is comparable across cells via an interactive crosshair.*

SOM Algorithm – We build upon Geo-SOM [BLP05], a SOM variant that restricts learning to a geographic vicinity. Bação et al. propose their method as a new SOM architecture for clustering and dimensionality reduction, but do not provide an interactive machine learning solution. The size of the geographic vicinity is controlled by an integer parameter k that specifies the number of output cells considered. At $k = 0$, only data points inside the corresponding map cell are considered, which makes the result equivalent to a gridded glyph map. As k increases, this geographic restriction is gradually relaxed, enabling a smooth transition towards a feature-driven SOM. Each spatial location is represented by its time series as an input vector, and the cell Best Matching Unit (BMU) is the codebook vector learned over these inputs.

Cell Design – While the BMU is a common cell representative, it alone does not capture the spatial extent and temporal variation of a cluster. We therefore use separate summaries for space and time in line with the duality of these two perspectives [AAB*10]. We use square cells because they align with the regular SOM lattice, support direct map overlay, and provide stable space for embedded summaries.

For *spatial summarization*, we display cell members as a scatterplot within the cell, normalized to their geographic bounding box so that relative spatial structure remains comparable across cells (see Fig. 1 (A)). This makes geographic concentration, spread, and outliers directly visible. Following the established effectiveness of 2D colormaps in SOM layouts [SKB*18], we overlay a 2D colormap (Ziegler et al. [ZNK07]) and color each member by its geographic position.

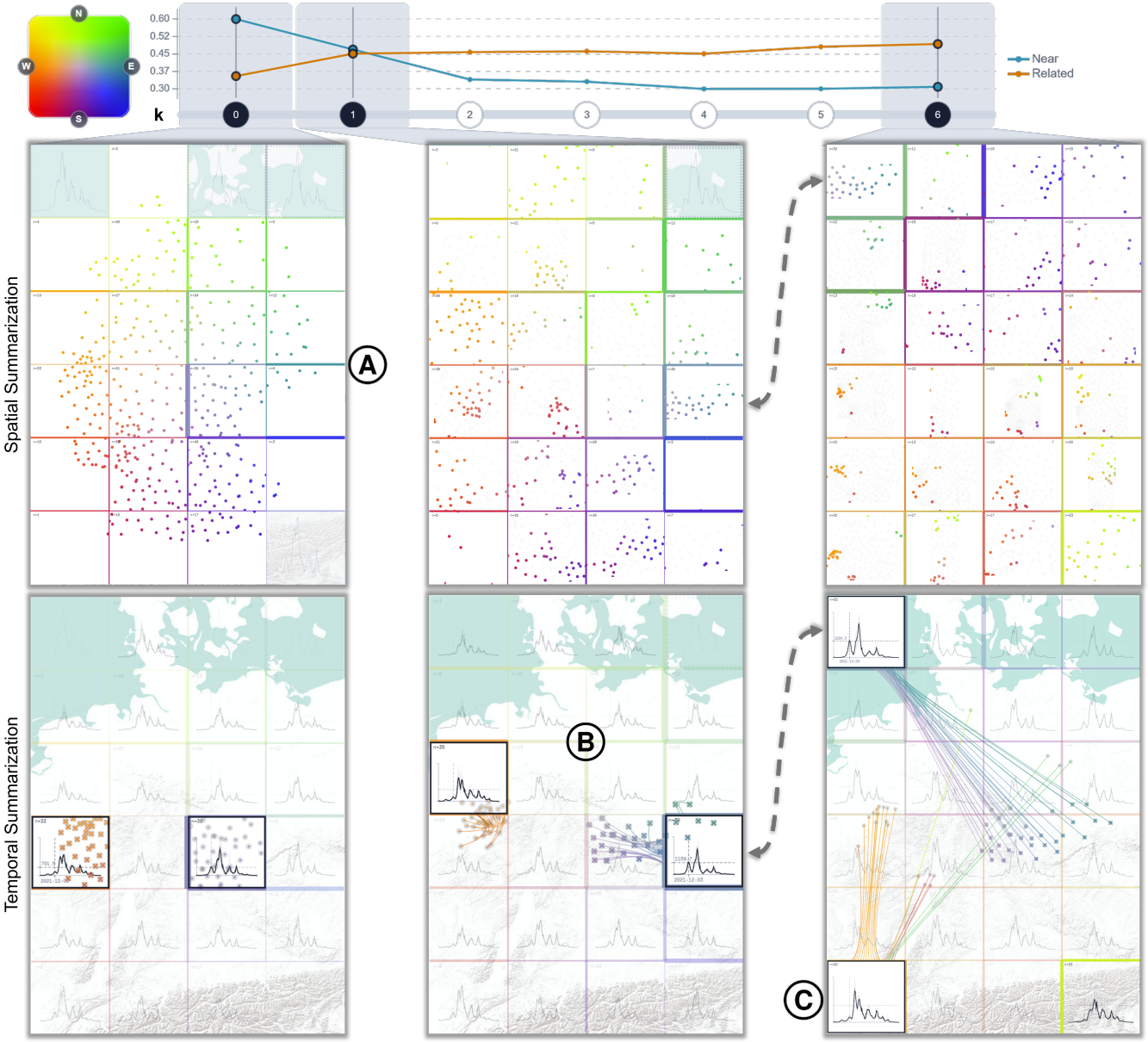

Figure 2: *Different values of k support different analysis tasks. Left: $k=0$ yields a gridded glyph map that allows for the inspection of local agreement and local deviation. Middle: $k=1$ balances geographic proximity and temporal similarity, combating MAUP while maintaining geographical coherence. Right: $k=6$ approaches a purely feature-driven SOM that can highlight remote similarities.*

Non-members within the bounding box are plotted in gray with reduced opacity, revealing whether a cell forms a compact local region or combines distant areas **`[T1,T3]`**.

For *temporal summarization*, we rely on traditional gridded glyph maps [WHWC12] and show a line chart for each cell (see Fig. 1 (B)). We display the BMU, the median, and the interquartile range to summarize representative behavior and within-cell variation. This supports comparison of coherent and deviating temporal developments. We chose a linear layout because it supports direct comparison of trends and deviations, a focus in our analysis, rather then a circular layout, following the approach by Slingsby et al. [SRH23]. Because the SOM preserves neighborhood relations in the similarity space, adjacent cells tend to represent similar temporal profiles. To make these transitions visible, we scale the width of the border between neighboring cells by the mean squared error between their BMUs. Thick borders therefore indicate stronger local change **`[T2]`**.

Map Linking – To achieve a single integrated view, we overlay the SOM grid on a geographic map. We follow the suggestion of Slingsby et al. [SRH23] to use a simple tile design to minimize visual interference. For larger k, cells are no longer directly bounded to the underlying geography and can drift away from the spatial locations of their members. We connect the cells to their members' geographical

locations using bundled lines to maintain geographic reference while reducing clutter (see Fig. 2 (C)).

Interaction – We provide a slider for k to steer the balance between geographic proximity and temporal similarity. To guide parameter selection, we summarize the geographic nearness and temporal relatedness measures across the possible k values and plot their weighted averages above the k slider (see Fig. 2 top). By default, cells show the spatial summary to preserve the geographic overview. On hover, we switch to the temporal summary and make the background transparent so that detailed temporal comparison remains possible without permanently obscuring the map, resembling a lens interaction. A given cell can be selected by clicking, enabling a crosshair that follows the mouse to compare temporal profiles across all other cells. Cells can further be filtered by geographic nearness and temporal relatedness using sliders. This supports the defined analysis tasks `[T1,T2,T3]` by focusing on cells with different combinations of geographic nearness and temporal relatedness.

4. Evaluation

The COVID-19 pandemic has produced large amounts of geolocated timeseries data that has previously been studied through gridded glyphmaps [SRH23]. We present a usage scenario using daily 7-day incidence per 100,000 inhabitants recorded across 400 German districts from 2020 to 2024 to evaluate our approach. Following the procedure described in Sec. 3, we train a 4×6 Geo-SOM with varying k over 10,000 stochastic iterations with an exponentially decaying learning rate ($0.5 \rightarrow 0.01$) and Gaussian neighborhood radius ($\sigma_0 = 1.5 \rightarrow 0.5$).

We start the analysis with $k = 0$, resembling a traditional gridded glyphmap, where wider cell borders can suggest local deviations between neighboring cells `[T2]`. In Fig. 2 (A), these deviations roughly align with the former inner German border, consistent with prior work that reports differing pandemic dynamics between eastern and western Germany [Die23]. However, some cells contain only a small number of districts and are located rather far away from the joint cell border, indicating susceptibility to the MAUP which is a known limitation of gridded glyphmaps [SRH23, LSJ24].

The measure summarization indicates that nearness and relatedness are balanced for $k = 1$ (Fig. 2), which relaxes the geographic constraint imposed on the grid. When filtering for high temporal relatedness, we observe two geographically compact clusters with similar temporal profiles `[T1]` (see Fig. 2 (B)). When inspecting the temporal profile lines using the crosshair, the more eastern cluster shows a pronounced wave in December 2021 followed by a weaker wave in February 2022 compared to the more western cluster.

When switching to $k = 6$, the cells form a classical SOM in which districts are grouped only by timeseries similarity. By focusing on cells with a high relatedness score, we can identify clusters with similar temporal profiles and inspect their geographic locations `[T3]`. One such cluster combines the urban regions of Hamburg, Berlin, Frankfurt, and the Ruhr area despite their geographic separation. This indicates that urban dynamics can outweigh plain spatial proximity in pandemic developments (see Fig. 2 (C)). The eastern German cluster remains visible at $k = 6$ in a different grid location, suggesting that its temporal pattern is robust even when geographic proximity no longer guides the grouping.

5. Discussion

By varying k interactively, we integrate the complementary advantages of geographically driven aggregation and similarity-driven grouping, thereby supporting the investigation of local agreement, local deviation, and remote similarity within a single analytical framework.

Cell Aggregation and Arrangement – For $k = 0$, the visualization inherits the MAUP-related limitations of gridded glyphmaps [SRH23, LSJ24], which can make differences between neighboring cells partly dependent on the aggregation layout. As shown in Sec. 4, this effect can be reduced by increasing k. However, larger k values weaken the geographic coupling of the SOM cells, so cells may drift away from their associated regions. In some cases, flipping or rotating the grid could improve the geographic coherence between the SOM layout and the map without losing the topographical structure of the SOM.

SOM Variant and Spatial Integration – We adopt the BMU-restricting k parameter from Bação et al. [BLP05] as it permits a bridging between gridded glyph maps and SOMs. Other ways of integrating spatial context, such as appending geographic coordinates to the feature vector, could be explored to study how cell drift manifests under alternative strategies. The temporal similarity is currently measured by Euclidean distance and is limited to aligned time series, but more refined options such as DTW-SOM [LSD*21] or relational SOM [OVV15] can replace it without affecting the visual encoding.

Cluster Stability – Some clusterings remain visible across a broad range of k, while others only appear at individual settings. This suggests that persistence across k may indicate more robust patterns, whereas short-lived clusters may be parameterization artifacts. A useful extension would track which clusters persist across k and where they split or merge, similar to stability-based hierarchical clustering approaches [CMZS15].

Visual Complexity – The integrated view combines embedded summaries, connecting links, border encodings, and geographic context in a single, complex representation. While this provides high information content, it is also susceptible to overplotting, especially in dense regions or for larger k. Additionally, the geographical context of the hovered cell is obscured by the corresponding summary plot due to the superimposition.

Cell Occupancy and Data Density – Meaningful spatial and temporal summaries require enough observations per cell to produce representative aggregates. If the grid is too fine or the dataset too sparse, cells may contain only a few members, weakening the interpretability of the embedded summaries and the nearness and relatedness measures, where established quantization error and topographic error could serve as complementary quality measures [KNH09].

6. Conclusion

We presented a visual analytics approach that combines gridded glyph maps and self-organizing maps for the analysis of spatiotemporal data. The superimposed view supports a continuous transition between spatial aggregation and similarity-based grouping, enabling the investigation of local agreement, local deviation, and remote similarity within a single interface. By combining spatial summaries, temporal summaries, and nearness and relatedness measures, the approach preserves geographic context while supporting comparison of temporal behavior. Our case study on German COVID-19 incidence data illustrates the proposed workflow in practice and its use for spatiotemporal analysis.

References

[AAB*10] ANDRIENKO G., ANDRIENKO N., BREMM S., SCHRECK T., VON LANDESBERGER T., BAK P., KEIM D.: Space-in-Time and Time-in-Space Self-Organizing Maps for Exploring Spatiotemporal Patterns. *Comput. Graph. Forum 29*, 3 (2010), 913–922. doi:10.1111/j.1467-8659.2009.01664.x. 1, 2

[BDHL21] BEECHAM R., DYKES J., HAMA L., LOMAX N.: On the Use of 'Glyphmaps' for Analysing the Scale and Temporal Spread of COVID-19 Reported Cases. *ISPRS Int. Journal of Geo-Information 10*, 4 (Apr. 2021), 213. Number: 4. doi:10.3390/ijgi10040213. 1

[BLP05] BAÇÃO F., LOBO V., PAINHO M.: The self-organizing map, the Geo-SOM, and relevant variants for geosciences. *Computers & Geosciences 31*, 2 (2005), 155–163. doi:10.1016/j.cageo.2004.06.013. 1, 2, 4

[BRS*12] BERNARD J., RUPPERT T., SCHERER M., SCHRECK T., KOHLHAMMER J.: Guided discovery of interesting relationships between time series clusters and metadata properties. In *Proc. Int. Conf. Knowl. Manage. and Knowl. Technol.* (2012), pp. 1–8. doi:10.1145/2362456.2362485. 2

[CHM18] CHIBA H., HYOGO Y., MISUE K.: Static Representation Exposing Spatial Changes in Spatio-Temporal Dependent Data. *IEICE Trans. Inf. Syst. E101.D*, 4 (2018), 933–943. doi:10.1587/transinf.2016IIP0021. 1

[CMZS15] CAMPELLO R. J. G. B., MOULAVI D., ZIMEK A., SANDER J.: Hierarchical Density Estimates for Data Clustering, Visualization, and Outlier Detection. *ACM Trans. Knowl. Discov. Data 10*, 1 (2015), 1–51. doi:10.1145/2733381. 4

[Die23] DIEBNER H. H.: Spatio-temporal patterns of the sars-cov-2 epidemic in germany. *Entropy 25*, 8 (2023). doi:10.3390/e25081137. 4

[DPL*19] DENNIG F. L., POLK T., LIN Z., SCHRECK T., PFISTER H., BEHRISCH M.: FDive: Learning Relevance Models using Pattern-based Similarity Measures. In *Proc. IEEE Conf. on Visual Analytics Science and Technology (VAST)* (2019), IEEE, pp. 69–80. doi:10.1109/VAST47406.2019.8986940. 2

[DYL*17] DU Y., YUAN C., LI B., HU W., MAYBANK S.: Spatio-Temporal Self-Organizing Map Deep Network for Dynamic Object Detection from Videos. In *IEEE Conf. Comput. Vision Pattern Recognit. (CVPR)* (2017), pp. 4245–4254. doi:10.1109/CVPR.2017.452. 2

[GCML06] GUO D., CHEN J., MACEACHREN A., LIAO K.: A Visualization System for Space-Time and Multivariate Patterns (VIS-STAMP). *IEEE Trans. on Vis. and Comp. Graph. 12*, 6 (2006), 1461–1474. doi:10.1109/TVCG.2006.84. 1

[GCS24] GUÉRIN A., CHAUVET P., SAUBION F.: A survey on recent advances in self-organizing maps. *arXiv preprint arXiv:2501.08416* (2024). 1, 2

[GG06] GUO D., GAHEGAN M.: Spatial ordering and encoding for geographic data mining and visualization. *J. Intell. Inf. Syst. 27*, 3 (2006), 243–266. doi:10.1007/S10844-006-9952-8. 2

[GW15] GROLEMUND G., WICKHAM H.: Visualizing complex data with embedded plots. *Journal of Computational and Graphical Statistics 24*, 1 (2015), 26–43. doi:10.1080/10618600.2014.896808. 1

[HRJ*13] HAO M. C., ROHRDANTZ C., JANETZKO H., KEIM D. A., DAYAL U., ERIK HAUG L., HSU M., STOFFEL F.: Visual sentiment analysis of customer feedback streams using geo-temporal term associations. *Inf. Visualization 12*, 3-4 (2013), 273–290. doi:10.1177/1473871613481691. 2

[KNH09] KOHONEN T., NIEMINEN I. T., HONKELA T.: On the Quantization Error in SOM vs. VQ: A Critical and Systematic Study. In *Proc. Int. Workshop on Advances in Self-Organizing Maps* (2009), WSOM '09, pp. 133—144. doi:10.1007/978-3-642-02397-2_16. 4

[Koh82] KOHONEN T.: Self-organized formation of topologically correct feature maps. *Biol. Cybern. 43*, 1 (1982), 59–69. doi:10.1007/BF00337288. 1, 2

[LSD*21] LI K., SWARD K., DENG H., MORRISON J., HABRE R., FRANKLIN M., CHIANG Y.-Y., AMBITE J. L., WILSON J. P., ECKEL S. P.: Using dynamic time warping self-organizing maps to characterize diurnal patterns in environmental exposures. *Scientific reports 11*, 1 (2021), 24052. doi:10.1038/s41598-021-03515-1. 4

[LSJ24] LAKSONO D., SLINGSBY A., JIANU R.: Gridded-glyphmaps for supporting Geographic Multicriteria Decision Analysis. In *EuroVis Short Papers* (2024). doi:10.2312/evs.20241062. 1, 4

[Ope84] OPENSHAW S.: The modifiable areal unit problem. *Concepts and techniques in modern geography* (1984). 2

[OVV15] OLTEANU M., VILLA-VIALANEIX N.: On-line relational and multiple relational SOM. *Neurocomputing 147* (2015), 15–30. doi:10.1016/j.neucom.2013.11.047. 4

[RDS*25] RAUSCHER J., DENNIG F. L., SCHLEGEL U., KEIM D. A., FUCHS J.: Visually Assessing 1-D Orderings of Contiguous Spatial Polygons. *Comput. Graph. Forum 44*, 3 (2025). doi:10.1111/cgf.70100. 2

[SKB*18] SACHA D., KRAUS M., BERNARD J., BEHRISCH M., SCHRECK T., ASANO Y., KEIM D. A.: SOMFlow: Guided Exploratory Cluster Analysis with Self-Organizing Maps and Analytic Provenance. *IEEE Trans. on Vis. and Comp. Graph. 24*, 1 (2018), 120–130. doi:10.1109/TVCG.2017.2744805. 2

[SRH23] SLINGSBY A., REEVE R., HARRIS C.: Gridded Glyphmaps for Supporting Spatial COVID-19 Modelling. In *IEEE Visualization and Visual Analytics* (2023), pp. 1–5. doi:10.1109/VIS54172.2023.00009. 1, 3, 4

[Tob70] TOBLER W. R.: A Computer Movie Simulating Urban Growth in the Detroit Region. *Economic Geography 46* (1970), 234–240. doi:10.2307/143141. 1

[WHWC12] WICKHAM H., HOFMANN H., WICKHAM C., COOK D.: Glyph-maps for Visually Exploring Temporal Patterns in Climate Data and Models. *Environmetrics 23*, 5 (2012), 382—393. 1, 3

[ZNK07] ZIEGLER H., NIETZSCHMANN T., KEIM D. A.: Visual Exploration and Discovery of Atypical Behavior in Financial Time Series Data using Two-Dimensional Colormaps. In *Inf. Visualization* (2007), pp. 308–315. doi:10.1109/IV.2007.124. 2

[ZP04] ZHANG X., PAZNER M.: The icon imagemap technique for multivariate geospatial data visualization: Approach and software system. *Cartogr. Geogr. Inf. Sci. 31*, 1 (2004), 29–41. doi:10.1559/152304004773112758. 1